Tunnelling and Underground Space Technology 140 (2023) 105298

Contents lists available at ScienceDirect

Tunnelling and Underground Space Technology incorporating Trenchless Technology Research

journal homepage: www.elsevier.com/locate/tust

# Auxiliary ventilation systems in mining and tunnelling: Air leakage prediction and system design to optimize the energy efficiency and operation costs

Javier Menéndez [a], Jesús M. Fernández-Oro [b,*], Noe Merlé [c], Mónica Galdo [b], Laura Álvarez [d], Cipriano López [e], Antonio Bernardo-Sánchez [d]

[a] Mining and Civil Department, Sadim Engineering, Oviedo 33005, Spain
[b] Fluid Mechanics Department, University of Oviedo, Gijón 33203, Spain
[c] Civil and Mining Engineering, TSK Group, Gijón 33203, Spain
[d] Department of Mining Technology, Topography and Structures, University of León, León 24071, Spain
[e] Tunnelling and Mining Department, ZITRON Ventilation Systems, Gijón 33211, Spain

ARTICLE INFO

*Keywords:*
Auxiliary ventilation
Tunnelling
Mining
Ventilation costs
Leaky ducts
Design

ABSTRACT

The excavation of tunnels and mining roadways requires auxiliary ventilation systems to dilute the noxious gases from blasting and diesel engines and provide a safe environment for workers. Therefore, axial fans and ducting systems are generally installed to supply the required airflow rate to the working face. Due to the air leakage, the airflow rate varies along the ventilation duct and the design of the ventilation system is complex when leaky ducts are used. Thus, to ensure the required airflow rate at the working face, a proper sizing of the ducting system and auxiliary fan must be carried out. In this paper, analytical and CFD numerical models have been conducted to investigate auxiliary ventilation systems considering different qualities of the ventilation ducts. A forced duct of 0.6 m in diameter and 200 m long in a 14 $m^2$ cross section mining roadway has been selected to predict the pressure drop and the air leakage along the duct. In addition, the power of the fan and the energy consumption have also been studied in the analytical models to optimize the energy efficiency and ventilation costs. The results obtained show that the power of the fan can be reduced by 74% if a duct 0.8 m in diameter is installed. Good agreements were obtained between the numerical approach and the analytical results. Finally, novel nomograms have been developed to design the ducting system and the auxiliary fans and estimate the energy consumption as a function of non-dimensional variables. Duct diameters between 600 and 2400 mm and tunnel lengths up to 4000 m can be selected to design the auxiliary ventilation circuits optimizing the operation costs.

## 1. Introduction

Auxiliary ventilation systems (Wallace et al., 2015) are required to provide a safe working environment for the workers in dead-end mining roadways and tunnels (Massanes et al., 2015; Parra et al., 2006). Axial fans are typically installed at the tunnel portal to supply fresh air to the working face through a ventilation duct (Auld, 2002). Electrical energy is required to supply fresh air by an axial fan during the excavation of tunnels and mining roadways, increasing energy consumption when the power of the fan increases (Auld, 2004). The airflow rate generally depends on the number of workers, power of the diesel engines operating simultaneously and the amount and type of explosives used in blasting operations (Menéndez et al., 2022). Toxic gases from blasting operations and diesel engines must be diluted using the auxiliary ventilation systems, reducing its concentration below the threshold limit value according to health and safety regulations (Lowndes et al., 2004; McPherson, 1993). Different ventilation modes can be employed, being the forced system the most used during the excavation of tunnels and mining developments (Xin, 2021). The fresh air supplied by the fan reaches the working face through the ventilation duct, while the dirty air returns towards the tunnel outside through the tunnel section (Chang et al., 2019). Depending on the tunnel length and amount of airflow rate at the end of the ventilation duct, the axial fan and the ducting system must be sized. Therefore, the power of the fan and the diameter of the

* Corresponding author.
*E-mail address:* jesusfo@uniovi.es (J.M. Fernández-Oro).

https://doi.org/10.1016/j.tust.2023.105298
Received 29 March 2023; Received in revised form 12 June 2023; Accepted 24 June 2023
Available online 27 June 2023

ventilation duct have to be properly calculated to supply the required fresh airflow to the working face (Vutukuri, 1993). Note that due to the increase in air pressure, the power of the fan increases strongly when the diameter of the ventilation duct decreases. Auxiliary ventilation systems are easy sized if the ventilation duct is free-leak (Gupta et al., 1987; Lee, 2017). However, leaky ducts are generally used during the excavation of tunnels and mining roadways and the design of the ventilation system is complex (Onder and Cevik, 2008). Due to air leakage the airflow rate varies along the ventilation duct until it reaches the working face. Depending on the rate of loss along the ducting system, the airflow rate at end of the duct can be lower than required. Air leakage is due to the quality of the ventilation duct (ruptures in the wall) and the presence of numerous joints in the ducting system (Auld, 2004). The quality of the ventilation ducts generally worsens due to the damage caused by blasting as well as by the mobile equipment that operates inside the tunnel (dumper trucks, excavators, jumbos, shotcrete machinery…). Different qualities of the ducts are considered according to the Swiss Standard SIA 196. Hence, S, A and B duct classes are considered depending on the active leakage surface and friction factors (SIA 196, 1998). The air leakage in the duct joints can be reduced if a suitable joint system is selected and proper installation is carried out (De Souza, 2004). The rate of loss along the ventilation duct increases in leaky ducts when the fan total pressure increases, reducing the airflow rate at the end of the duct. Increasing the diameter of the ventilation duct, the rate of loss is reduced along the ducting and the airflow rate increases in the tunnel face. In addition, the energy costs are also reduced by increasing the duct diameter, decreasing the fan pressure (De Souza, 2018). However, the increase of duct diameter is difficult in many cases due to the available cross-sectional area. The design of the excavation cross-sectional area is carried out based on the diameter of the ventilation duct, especially in mining developments. Sufficient clearance between the ducting and the mobile equipment must be considered to avoid damage to the air duct (De Souza, 2004). Hence, it is essential to carry out an adequate analysis of the auxiliary ventilation systems to ensure the required airflow rate at the working face and optimize investment and energy costs during the excavation of tunnels and mining roadways (Dang et al., 2021; Dang and Bui, 2020; De Vihena and Margarida, 2020).

Many researchers have investigated the auxiliary ventilation systems in underground excavations. Onder et al., 2006 developed a computer program to analyze the influence of ventilation variables on the airflow provided to the working face. They carried out field measurements in an underground coal mine and concluded that the increase of duct diameter is the key to ensure the adequate airflow to the heading face. Auld, 2004 carried out a fan performance considering leaky ventilation ducts. He used the Atkinson equation to analyze the sensitivity of a leak-free duct considering different duct diameters, friction factors and airflow and defined an equation to estimate the air leakage from a ventilation duct as a function of a leakage coefficient, a nominal duct surface area (1000 $m^2$), and a reference differential static pressure of 1000 Pa. Similarly, to evaluate the air leakage, Vutukuri, 1983 and Onder, 2000 employed a leakage coefficient defined as $m^3\ s^{-1}$ of air leakage per 100 m of duct under a uniform pressure of 1 kPa. A design procedure for auxiliary ventilation systems considering leakage was presented by Vutukuri, 1984. He analyzed the installation of the fan to avoid recirculation of dirty air in the ventilation circuit. Millar et al. (2017) analyzed the air leakage through the joints between duct segments in auxiliary ventilation systems to improve the efficiency and reduce the ventilation costs. They considered leaky systems with a low duct joint resistance of 104 $Ns^2\ m^{-8}$ for each joint and non-leaky systems with duct joint resistances per joint of 107 $Ns^2\ m^{-8}$. Auxiliary ventilation systems with variable and fixed speed fans were investigated. They concluded that the cost of ventilation system could be reduced by using a ducting system with lower Atkinson friction factor and selecting a duct system with non-leaky couplings. De Souza, 2004 studied the air leakage in ducting system and estimated an air leakage of 0.9 $m^3\ s^{-1}$ per each joint. However, it is not specified the range of pressure and duct diameter and friction factor. Leakage resistance values in long auxiliary ventilation systems were estimated using the same length and duct diameter and varying the fan pressure and airflow (Calizaya and Mousset-Jones, 1993, 1994, 1997). Although different resistance values were calculated for each trial, a constant value should have been obtained considering the same ducting system. A comprehensive design process for auxiliary ventilation systems is presented in Duckworth and Lowndes, 2003. An engineering software to design the auxiliary fan and the ducting system was developed to optimize the auxiliary ventilation systems in mines and tunnels. Different duct material and diameter, number and spacing of axial fans and shock losses can be selected to improve the system efficiency. Gillies and Wu, 1999 conducted field measurements on 0.45 and 0.915 m duct diameter and 100 m long using electronic pressure transducers to determine the friction factor and air leakage. Atkinson friction factors of 0.0021 and 0.0041 $Ns^2\ m^{-4}$ were obtained for light-weight and heavier material, respectively. Kosowski et al., 2022 investigated the air leakage in a forced air duct for the excavation of an underground tunnel using CFD simulation. They considered 300 m long and 1 m diameter ducting system with a 55 kW axial fan. The wall roughness was investigated by Zhang et al., 2022 both experimentally and numerically, to determine the influence on the ventilation resistance coefficient during the excavation of tunnels.

Researchers also investigated the influence of the auxiliary ventilation systems on the propagation and dilution of toxic gases in underground excavations after blasting operations. The auxiliary ventilation system was studied after blasting operations in an underground coal mine by Torno et al., 2013. A CFD analysis was conducted to evaluate the evolution of CO concentration after blasting. Menendez et al., 2022 studied the concentration, propagation and dilution of hazard gases after blasting during the excavation of a railway tunnel. They conducted analytical and three-dimensional CFD numerical models to predict the propagation of toxic gases considering different ventilation modes. The results obtained were validated with field measurements. Diego et al., 2011 also investigated the air pressure loss in a mine tunnel using CFD modelling. Huang et al., 2020 analyzed the propagation of CO after blasting in a plateau mine under forced ventilation system. They analyzed the effect of altitude, ventilation volume and distance between duct mouth and working face and concluded that the CO concentration produced after blasting operations was most affected by the distance between end of the ventilation duct and heading face. A ventilation system using both blowing and exhaust ducts was conducted by Yi et al., 2020 using CFD simulation in a 36 m long and 2.9 m high mining tunnel. They concluded that the use of both forced and exhaust ventilation ducts is effective to provide the required fresh air to the working face. Bahrami et al., 2019 studied the re-entry time after blasting in a limestone mine using gas monitoring. They concluded that the use of gas monitoring can be useful to reliably determine the re-entry time and reduce the risk for workers. Torno and Toraño, 2020 investigated the toxic gases behavior after blasting in underground coal mines using CFD models and field measurements. The CO and $NO_2$ concentration was evaluated to estimate the safe re-entry time. Toraño et al., 2009 carried out a CFD study to predict the concentration and flow rate of methane in an underground coal mine. They analyzed the auxiliary ventilation system and concluded that can be effective to reinforce the forced system with exhaust overlap, jet fans or compressed air injectors (Toraño et al., 2011). A CFD analysis was conducted by Lee, 2011 to determine the diameter and position of the air duct to optimize the ventilation of the working face in a limestone mine.

In this paper, auxiliary ventilation systems in mining and tunnelling are investigated to optimize the energy efficiency and ventilation costs. One-dimensional analytical and CFD numerical models have been conducted in dead-end tunnels to analyze the pressure drop and air leakage along the leaky ventilation ducts. According to the Swiss Standard SIA 196, three different classes of ducts in relation to their quality were considered: S, A and B classes. Depending on the class of duct, different

leakage parameters (active leakage surface per duct surface) and friction factors have been considered. Leakage parameters of 5, 10 and 20 $mm^2$ $m^{-2}$ and constant friction factors of 0.015, 0.018 and 0.024 are considered for S, A and B classes, respectively, according to SIA 196 These coefficients can be determined specifically for each scenario from the numerical models depending on the duct quality and operating airflow rate. A forced ventilation duct of 0.6 m in diameter and 200 m long in a mining tunnel has been considered as a case study to predict the leakage and airflow at the working face depending on the class of duct. The models developed allow sizing the ducting system and fan power to optimize the energy efficiency and ventilation costs. The results obtained in the one-dimensional analytical model have been validated with the CFD model. In addition, the results have also been compared to other existing research works in the literature. Finally, novel nomograms have been developed to design the auxiliary ventilation systems in mining and tunnelling. Non-dimensional variables defined as power coefficient and energy coefficient have been determined to design the ducting system and the auxiliary fans depending on the duct class, tunnel length, airflow rate at the working face, tunnel altitude and fan efficiency. In order to select the most efficient solution, the energy consumption has also been estimated considering a utilization factor of the fan and the efficiencies of the motor and variable frequency drive.

## 2. Methodology

### 2.1. Problem statement

Ventilation systems are required during the construction of tunnels and mining roadways to provide a safe environment for workers and dilute the blasting fumes and combustion gases from diesel equipment (Parra et al., 2006). In addition, according to the international regulations, a minimal air speed in the underground infrastructure must also be guaranteed. The schematic diagram of a typical auxiliary ventilation system of dead-end tunnels and mining roadways is shown in Fig. 1.

The ducting system and auxiliary fan must be sized to ensure the required airflow to the working face. However, to design the ducting system, the size of the tunnel and mobile equipment must be considered to allow sufficient clearance between the vent duct and mobile equipment. The axial fans are located at the tunnel portal to avoid the recirculation of dirty air in the ventilation circuit. The power of the fans depends on the total pressure and the delivered airflow. Forced ventilation modes with leaky flexible ducts are generally used to supply fresh air directly to the working face in dead-end tunnels. The dirty air returns towards the tunnel portal through the tunnel section.

The problem statement is formulated as shown in Fig. 2. A leaky ventilation duct, 200 m in length and 0.6 m in diameter, with 10 uniformly distributed leakage points in a forcing system is considered. A fan total pressure is applied at the inlet of the duct as a boundary condition. The airflow does not vary in leak-free ducts ($Q_w = Q_f$). However, the airflow is lower in the working face when leaky ducts are used in auxiliary ventilation systems ($Q_w < Q_f$). The frictional pressure loss is caused by friction between the air and duct wall and the airflow rate and dynamic pressure decrease along the duct due to air leakage. Therefore, the pressure drop, air leakage along the duct and airflow rate at the end of the duct are investigated using analytical and CFD numerical models considering different classes of ventilation ducts. In order to optimize the energy efficiency, different duct diameters are also analyzed to estimate the air leakage and the power of the fan in each scenario.

Table 1 shows three different classes of ventilation ducts in relation to their quality according to the Swiss Standard SIA 196 (SIA 196, 1998). Friction factor, active leakage surface and unit surface leakage are considered for three duct classes S, A and B to predict the pressure drop, the air leakage and the airflow rate at the working face. S class is a new, properly mounted and regularly maintained duct, with segments longer than 100 m and few connections (very low leakage and friction losses). A class is a new, properly mounted with low duct damage risk (low air leakage and friction losses). Finally, B class is a duct already in operation or it is being used with regular maintenance. The unit surface leakage is calculated for each duct class considering a total duct surface of 377 $m^2$ and 10 air leakage points along the ventilation duct 200 m long and 0.6 m in diameter.

### 2.2. Analytical model

The longitudinal evolution of the pressure along the ventilation duct, as well as distribution of the leakage flow rate and bulk velocities have been resolved numerically from the one-dimensional equation (ODE) system composed by Eq. (1) and Eq. (2).

$$\frac{du}{dx} = \frac{4f^{'}}{D}\sqrt{\frac{2p}{\rho(1+\zeta)}} \tag{1}$$

$$\frac{dp}{dx} = \frac{\lambda}{D}\rho\frac{u^2}{2} \tag{2}$$

where $u$ is the local bulk velocity in the duct (m $s^{-1}$), $D$ is the duct diameter (m), $\lambda$ is the friction factor (-), and $p$ is the static pressure of the air (Pa) (with density $\rho$) at every longitudinal position $x$ of the duct. In addition, $f^{'}$ represents, according to the SIA standard (SIA 196, 1998) the leakage parameter accounted as the ratio of the estimated leakage surface with respect to the total surface of the duct, whereas $\zeta$ holds for a characteristic coefficient of minor losses, typically around 0.3 (SIA 196, 1998). This coefficient also includes the fan losses (protected mesh screen, tubular silencer and transition piece). The first equation establishes a simple balance between the longitudinal velocity decay and the radial leakage velocity (driven by the local static pressure); while the second equation stands for the classic D'Arcy-Weisbach expression for major losses in conduits.

For a required value of discharged flow rate at the final end of the

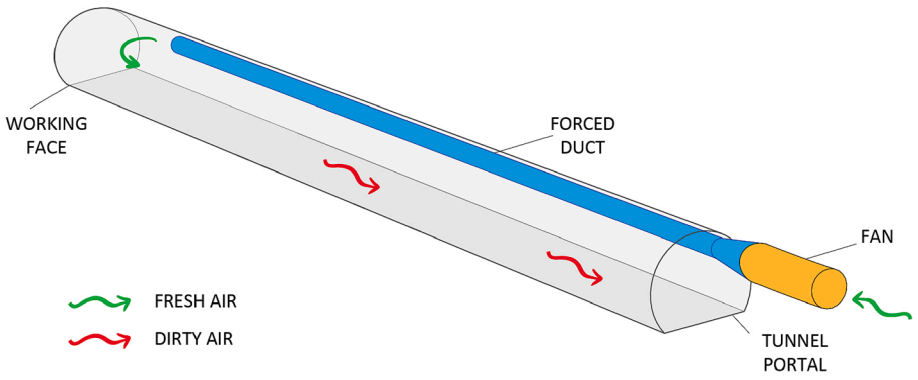


**Fig. 1.** Schematic diagram of a typical auxiliary ventilation system of dead-end tunnels and mining roadways.

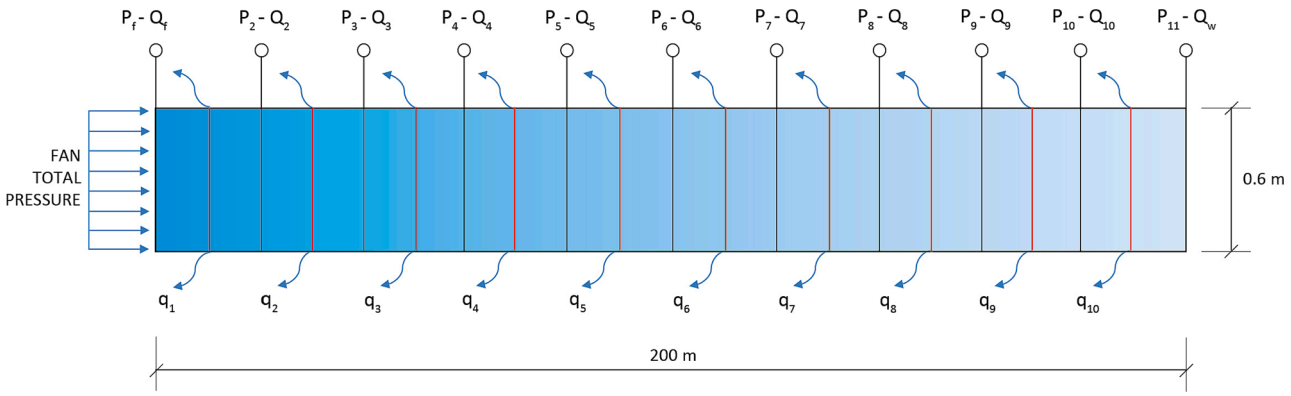


**Fig. 2.** Leaky duct, 200 m long and 0.6 m in diameter, in the forcing ventilation system.

**Table 1**
Different ventilation ducts classes (SIA 196, 1998).

| Duct Class | Friction coefficient, λ (-) | Active leakage surface, f′ ($mm^2\ m^{-2}$) | Unit surface leakage ($mm^2$) |
|---|---|---|---|
| S | 0.015 | 5 | 189 |
| A | 0.018 | 10 | 377 |
| B | 0.024 | 20 | 743 |

duct ($Q_w$), imposed as a boundary condition for the discharge velocity in Eq. (1), and an expected static pressure at the ventilated section of the tunnel for the boundary condition in Eq. (2), (assumed atmospheric, i.e, $p = 0$, manometric), the forth-order Runge-Kutta method was sequentially employed within the MATLAB code to resolve the equation system. Moreover, since the interest is placed on the initial flow rate required for the fan to assure the net flow rate at the working face, an additional iterative routine was implemented in the numerical modelling. The convergence threshold was fixed to the typical value $10^{-3}$, which in the worst cases, required around 10,000 iterations to achieve the final solution (for a representative situation of N = 10 leakage points). The model provides, as a function of the number of leakage positions (equally spaced), the pressure and velocity distributions, $p(x)$ and $u(x)$, along the vent duct.

The frictional pressure drop along the tunnel in the return circuit towards the exit can be calculated as a leak-free duct using Eq. (3) (Le Roux, 1979). The pressure drop in the tunnel is normally negligible compared to the pressure in the ventilation duct.

$$\Delta P = \frac{K \bullet C \bullet L \bullet Q^2}{A^3} \frac{\rho_{actual}}{\rho_{standard}} \tag{3}$$

where $\Delta P$ is the pressure drop in the return circuit (Pa), $K$ is the Atkinson friction factor (kg $m^{-3}$), depending on the type of tunnel and support system, being 0.014 kg $m^{-3}$ for arch-shaped tunnels with rock bolts and mesh as support system (Mc Pherson, 1993), $C$ is the perimeter of tunnel (m), $L$ is the length of tunnel (m), $Q$ is the airflow rate in the return circuit towards the tunnel outlet ($m^3\ s^{-1}$), $A$ is the cross sectional area of tunnel ($m^2$), $\rho_{actual}$ is the density of air (kg $m^{-3}$), $\rho_{standard}$ is the density of standard air (1.2 kg $m^{-3}$).

### 2.3. Numerical modelling

The CFD software ANSYS Fluent R17.0 was used to simulate airflow rate inside the ventilation duct. A two-dimensional model was developed to simulate the axisymmetric air flow inside the duct. Structured grid was generated in order to discretize the numerical domain considering 10 leakage points along the duct (duct connections and ruptures in the wall are simulated). Fig. 3 shows some details of the mesh and the zone where the grid was refined to accurately capture the physical phenomenon. As in the analytical model, a ventilation duct 200 m long and 0.6 m in diameter has been considered as a case study. As indicated in Table 1, a B class duct with a leakage surface of 743 $mm^2$ has been simulated.

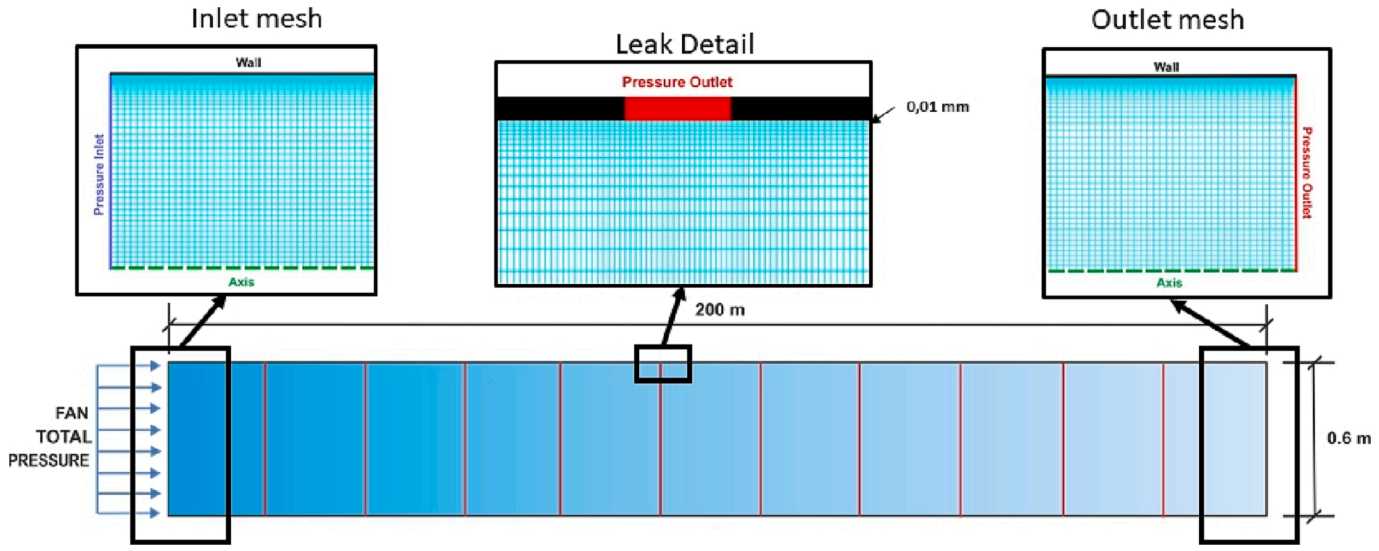


**Fig. 3.** Model grid and boundary conditions.

In addition, air flow in a ventilation duct is significantly affected by the walls, where the regions of viscosity have large gradients in the solution variables. An accurate representation of the region near the wall determines a successful prediction of wall-bounded turbulent flows. Therefore, a turbulent *k-ω* SST model was used to simulate the flow within the vent duct and a y + around 1 was imposed to deal with near-wall region velocity gradients. Vijiapurapu and Cui, 2010 demonstrated that regular RANS turbulence models, like k–ε, k–*ω*, or Reynolds stress models (RSM), as well as filtered Navier–Stokes equations along with Large Eddy Simulation (LES), perform equally well in predicting the time-averaged flow statistics to study the fully-developed turbulent flow in circular pipes. The k-*ω* SST model avoids the use of enhanced wall treatment characteristics from classic k-ε family models, reducing the modelling issues. To achieve the y+, the first cell of the model was placed at a distance of 0.01 mm from the wall. In summary, a total number of 2.3 M cells, with a [3000x75] cell distribution for every segment between the leakage joints, was selected. The main parameters of the numerical model conducted in Ansys Fluent are summarized in Table 2.

In order to simulate the pressure increase produced by the fan, a pressure inlet condition is imposed in the duct inlet. On the other hand, the discharge of the ventilation duct and the exit of the air through the cracks occurs at atmospheric pressure, therefore a condition of atmospheric pressure is imposed on all the outlets of the domain. Also, a non-slip boundary condition is fixed at the duct walls.

### 2.4. Nomograms of auxiliary ventilation systems for tunnelling and mining

Finally, in order to optimize the energy efficiency and operation costs, novel nomograms have been developed to design the ducting system and auxiliary fans considering leaky ducts in forcing systems. The power of the fan is calculated as a function of class of duct (quality), tunnel length, airflow rate at the working face, duct diameter, tunnel altitude and fan efficiency. Tunnels lengths up to 4000 m and duct diameters between 600 and 2,000 mm are considered in the nomograms. The power consumption is determined considering a time operation of 20 h day$^{-1}$ and efficiencies of the motor and variable frequency drive of 0.97 and 0.965, respectively (IEC, 2014).

### 2.5. Model validation

The results obtained in the 1D model have been validated with the CFD simulation. Fig. 4a shows the static pressure along the ventilation duct 200 m long and 0.6 m in diameter for a B class duct. Fig. 4b depicts the air leakage flow rate, in percentage with respect to the inlet flow rate, at every leakage joint. An airflow rate of 10 m$^3$ s$^{-1}$ is considered at the working face. As it can be seen in Fig. 4, good agreements were reached between both 1D analytical model and CFD numerical results.

To validate the accuracy of the computational mesh, the non-dimensional velocity distribution of the streamwise velocity ($u^+$) along the radial coordinate in wall units ($y^+$), in the case of a free-leak duct, has been compared to the empirical correlations which are well-documented in the literature (Pope, 2000). In particular, Fig. 5a shows a full match in the inner region of the boundary layer ($y^+ <300$) between the CFD results (black dots) and the universal law of the wall (red line), including the viscous sublayer ($y^+ <5$) through the classic blending equation provided by Van Driest (White, 2005). Precisely, this agreement confirms that the mesh distribution adopted is sufficient to resolve the wall-shear flow and guarantees the value of $y^+ \sim 1$. As the distribution evolves towards the duct center ($y^+ >300$), there is a progressive deviation which is also in complete concordance with the expected trends from the bibliography. Hence, in the outer part of the boundary layer (>20% δ, being δ the width of the boundary layer, i.e. the radius of the duct), the universal logarithmic law is no longer valid, with the classic Coles' law of the deficit for the velocity prevailing instead (blue line), as also confirmed by the CFD results. Note that no experimental values are available for the velocity profile in case of leakage ducts. However, this figure demonstrates that the high-dense meshes employed for the pipe flow are capable to reproduce with high fidelity the time-averaged wall-shear flow in the perpendicular direction, in case of high Reynolds numbers for smooth pipes. In addition, it has been introduced a progressive mesh along the axis direction (up to 3000 mesh nodes for every segment), which is also clustered towards the circumferential rings simulating the radial leakages (0.04 mm in length). Moreover, it has been carefully selected to present an accurate and high-quality discretization, with similar characteristics and cell sizes to the perpendicular direction ($x^+ \sim 1$).

The results obtained have also been validated with other existing research works in the literature. Fig. 5b shows a comparative analysis of the variation of the airflow rate along a ventilation duct 1000 m long and 915 mm in diameter. The model developed in this study to predict the quantity of air delivered to the working face has been compared to the British National Coal Board leakage nomogram and the experimental models developed by Vutukuri, 1983 and Gillies and Wu, 1999. As seen in Fig. 5, good agreements have been obtained.

**Table 2**
Parameters of the numerical model.

| Numerical model | Parameter |
|---|---|
| Solver | Pressure-based with PISO velocity coupling |
| Model | 2D Axisymmetric - Steady |
| Spatial discretization | First-order upwind |
| Gradient calculation | Least-squares cell-based |
| Turbulence model | k-ω SST |
| Cells number | 2.3 million |
| Convergence criteria | $10^{-10}$ |

## 3. Results and discussion

### 3.1. Analytical model results

The analytical model has been applied to analyze an auxiliary ventilation system in a dead-end mining roadway 14 m$^2$ cross section. A leaky ventilation duct 200 m long and 0.6 m in diameter has been considered to predict the air leakage and the required pressure at the fan outlet to ensure an airflow rate of 10 m$^3$ s$^{-1}$ at the working face ($Q_w$). Fig. 6a shows the bulk velocity along the duct for the three duct classes. Similarly, Fig. 6b represents the reduction of static pressure inside the duct. In order to take over the expected leakage, an airflow of $Q_f$ = 10.47 m$^3$ s$^{-1}$ is required for the fan at the tunnel inlet section when a B class duct (duct in operation) is considered ($f^* = f'/\sqrt{1+\zeta} = 20mm^2m^{-2}$ and $\lambda = 0.024$). The static pressure reaches 6250 Pa (total pressure of 7310 Pa) at the fan discharge. Considering a typical fan efficiency of 0.75, a power of the fan of 103 kW is obtained. The required airflow and pressure at the outlet of the fan decrease when better quality ducts are used.

In order to optimize the design of the ventilation circuit, the model has been solved for the three duct qualities considering a ventilation duct 0.8 m in diameter. Fig. 7a represents the longitudinal velocity along the duct and Fig. 7b shows the pressure drop from the fan to the working face. Compared to the scenario indicated in Fig. 6, a significant pressure reduction at the outlet of the fan was obtained, reaching 1460 Pa (total pressure of 1793 Pa) for B class ducts (red line). Therefore, the power of the fan decreases down to 25 kW, representing a reduction by 74%. The size of the mining roadway and mobile equipment should be considered to select the adequate ducting system in each case. An increase in the size of the mining roadway allows the installation of a larger diameter duct but significantly increases the excavation costs.

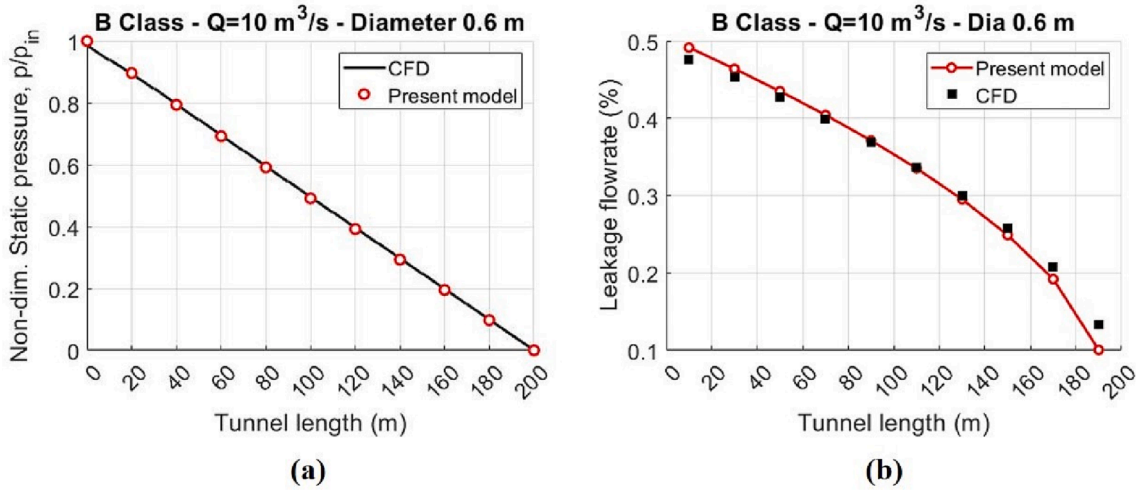


**Fig. 4.** Model validation. Comparative analysis between analytical and CFD results for a B class duct. (a) Static pressure along the 200 m duct; (b) Air leakage flow rate along the ventilation duct.

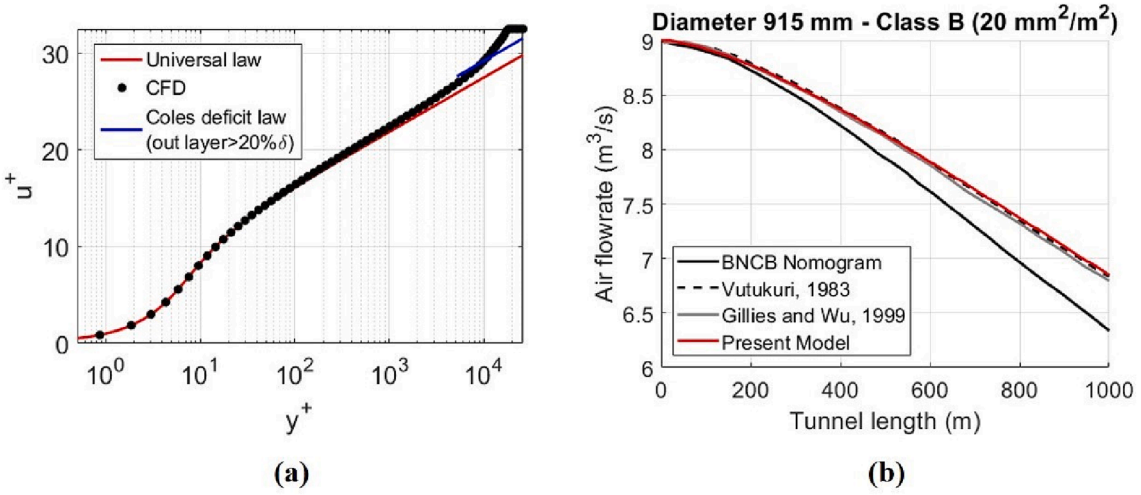


**Fig. 5.** Model validation. (a) Full match in the inner region of the boundary layer ($y^+<300$) between the CFD results and the universal law of the wall; (b) Air leakage along a ventilation duct 1000 m long and 0.915 m in diameter.

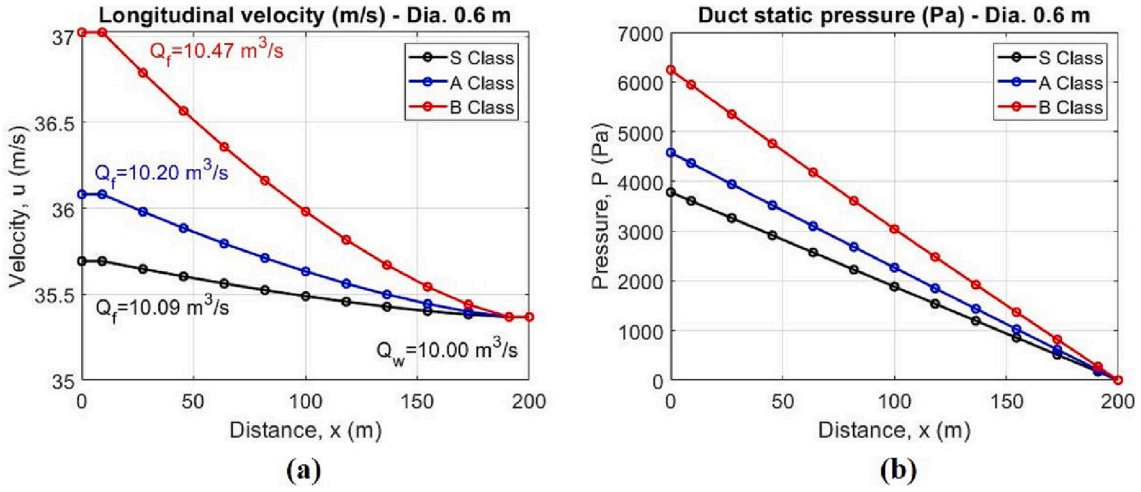


**Fig. 6.** Analytical results considering a leaky duct 200 m long and 0.6 m in diameter. (a) Longitudinal velocity along the duct and airflow at the working face; (b) Evolution of the static pressure for the three duct classes.

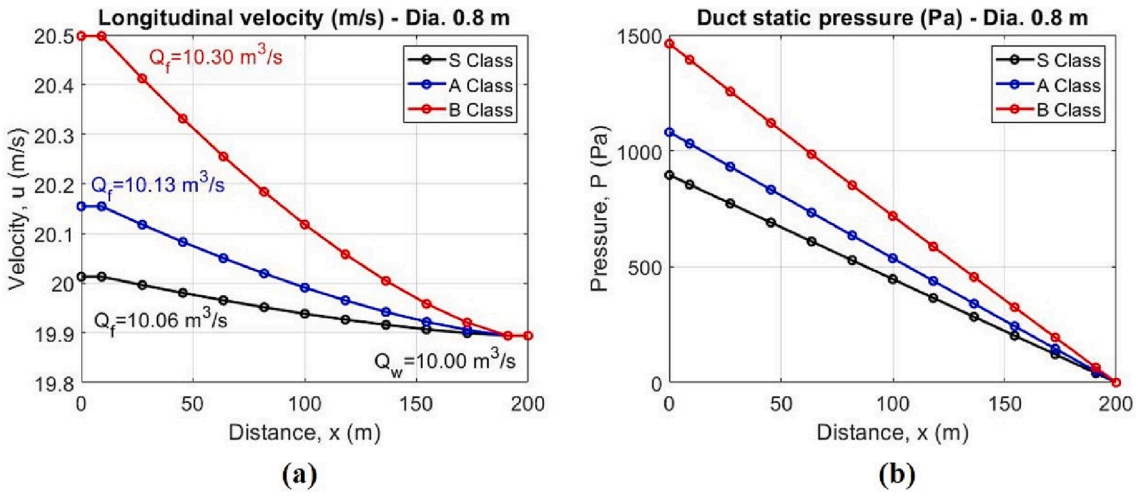


**Fig. 7.** Analytical results considering a leaky duct 200 m long and 0.8 m in diameter. (a) Longitudinal velocity along the duct and airflow at the working face; (b) Evolution of the static pressure for the three duct classes.

### 3.2. Numerical model results

To validate the results of the analytical model, a CFD numerical model has been performed. Fig. 8 shows the velocity vectors in three different leakage points along the duct. As it can be seen, the air velocity reaches 65 m $s^{-1}$ at the first point and decreases to 32 and 19 m $s^{-1}$ as the flow approaches the end of the tube. The pressure drop and the air leakage in each leakage joint are presented in Fig. 4, showing good agreements with analytical model.

### 3.3. Nomograms of auxiliary ventilation system

The model developed in this study has been applied to investigate the variation of the airflow rate along the ventilation duct in order to predict the airflow delivered to the working face. The size of the ducting system and auxiliary fan is essential to optimize energy consumption and ventilation costs. The air leakage and the power of the fan are estimated considering different duct classes and tunnels lengths up to 4000 m. Fig. 9 shows the analysis of forced ventilation systems considering S class with duct diameters of 800, 1400 and 2000 mm. Different values of airflow for the fan are considered depending on the duct diameter. Red lines represent the variation of the airflow rate from the fan discharge to the working face depending on the tunnel length. Black lines represent the fan power in kW for the different fan operating flow rates in $m^3$ $s^{-1}$. The air velocity and the total pressure increase strongly when the diameter of the duct decreases (Fig. 9a). Hence, to avoid problems in the duct during the operation the air velocity inside the duct must be limited. The power of the fan is calculated on a logarithmic scale considering a typical fan efficiency of 0.75 and an air density of 1.2 kg $m^{-3}$ (black y-axis in the plots).

Fig. 10 and Fig. 11 represent the nomograms of auxiliary ventilation systems considering A and B duct classes with active leakage surface of 10 and 20 $mm^2$ $m^{-2}$ and friction factors of 0.018 and 0.024, respectively. The results obtained show that the airflow delivered to the working face decreases as the length of the duct increases. The air leakage increases strongly in low quality ducts. In addition, due to the increase in pressure inside the duct, the delivered airflow rate also decreases when the duct diameter is reduced. The power of the fan is directly proportional to the total pressure and the airflow delivered by the fan. Considering the same airflow, the fan power decreases strongly

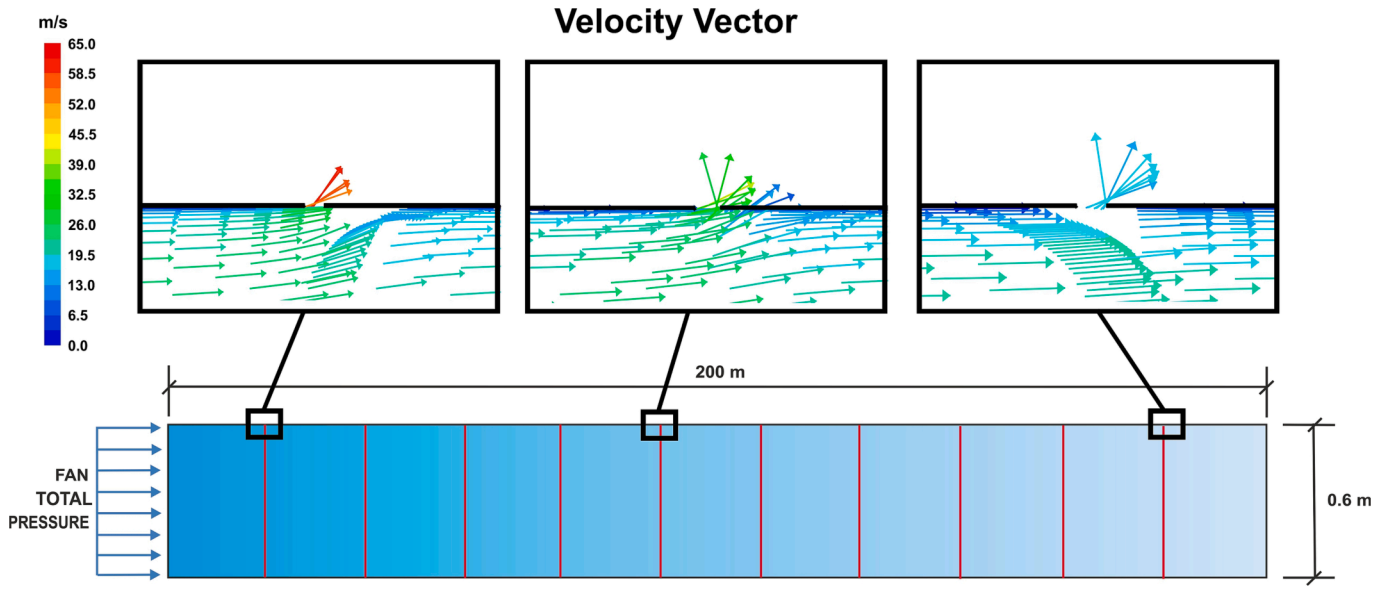


**Fig. 8.** Velocity vectors on the leakage points along the ventilation duct.

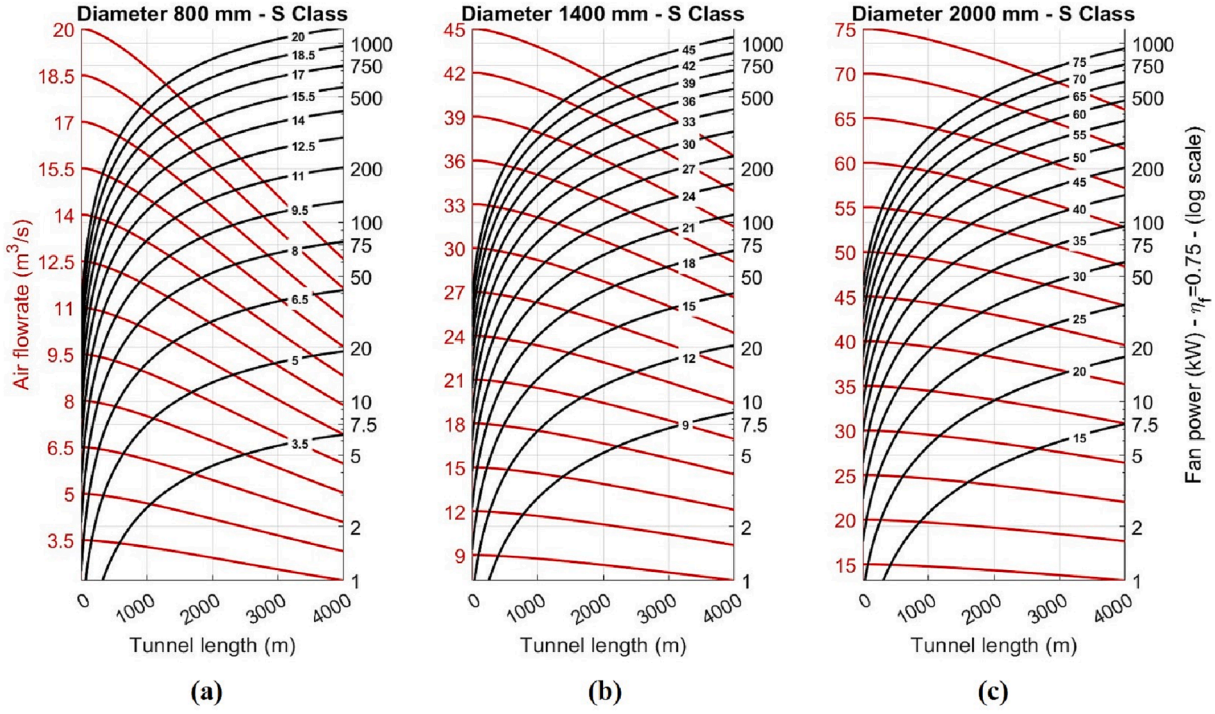


**Fig. 9.** Air leakage along the duct and fan power design for S class ducts considering tunnel lengths up to 4000 m and different duct diameters. (a) 800 mm; (b) 1400 mm; (c) 2000 mm.

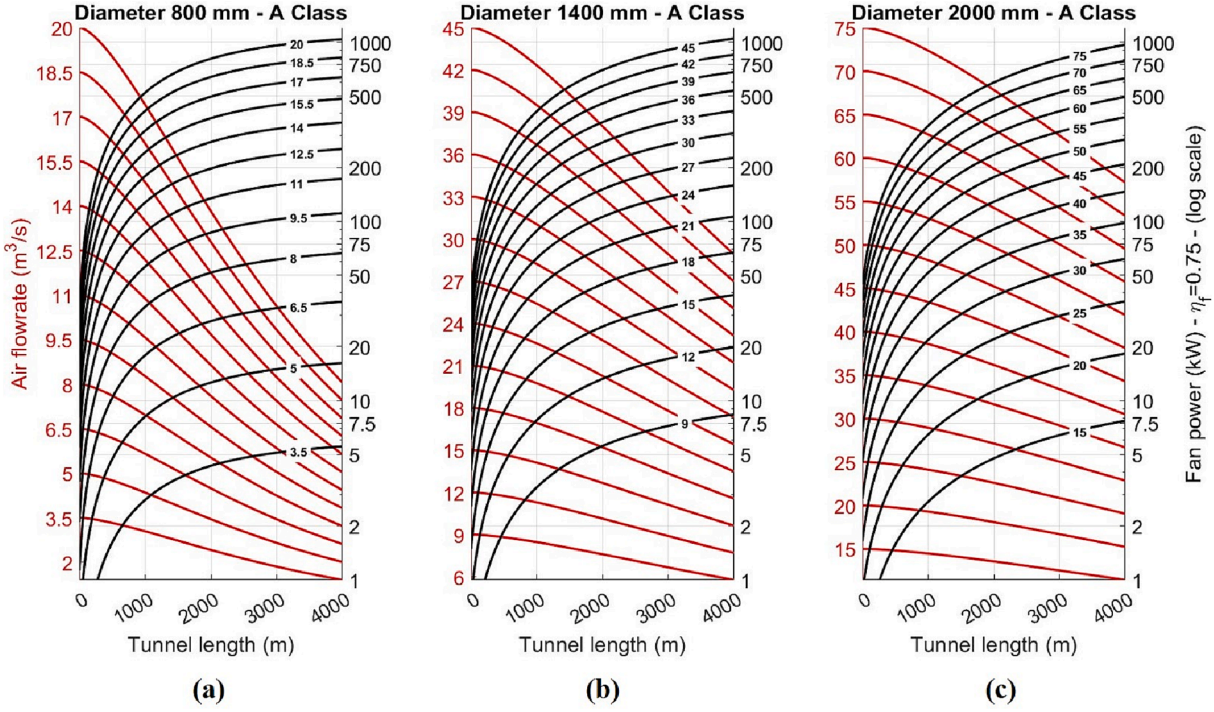


**Fig. 10.** Air leakage along the duct and fan power design for A class ducts considering tunnel lengths up to 4000 m and different duct diameters. (a) 800 mm; (b) 1400 mm; (c) 2000 mm.

when a smaller diameter duct is installed. However, the diameter of the duct could be limited by the size of the tunnel and the mobile equipment. The increase in the duct diameter would imply an increase in the size of the excavation section, implying a significant increase in investment costs. Considering a B class duct of 1250 m in length with an airflow at the fan exit of 21 $m^3\ s^{-1}$, the power of the fan reaches 770 kW with a duct 0.8 m in diameter. The fan power decreases down to 65 kW and 12 kW for duct diameters of 1.4 and 2 m, respectively.

Finally, novel nomograms have been developed to design auxiliary ventilation systems in mining and tunnelling and optimize the energy efficiency and ventilation costs using forced modes and flexible leaky ducts. Two non-dimensional variables defined as power coefficient (ξ)

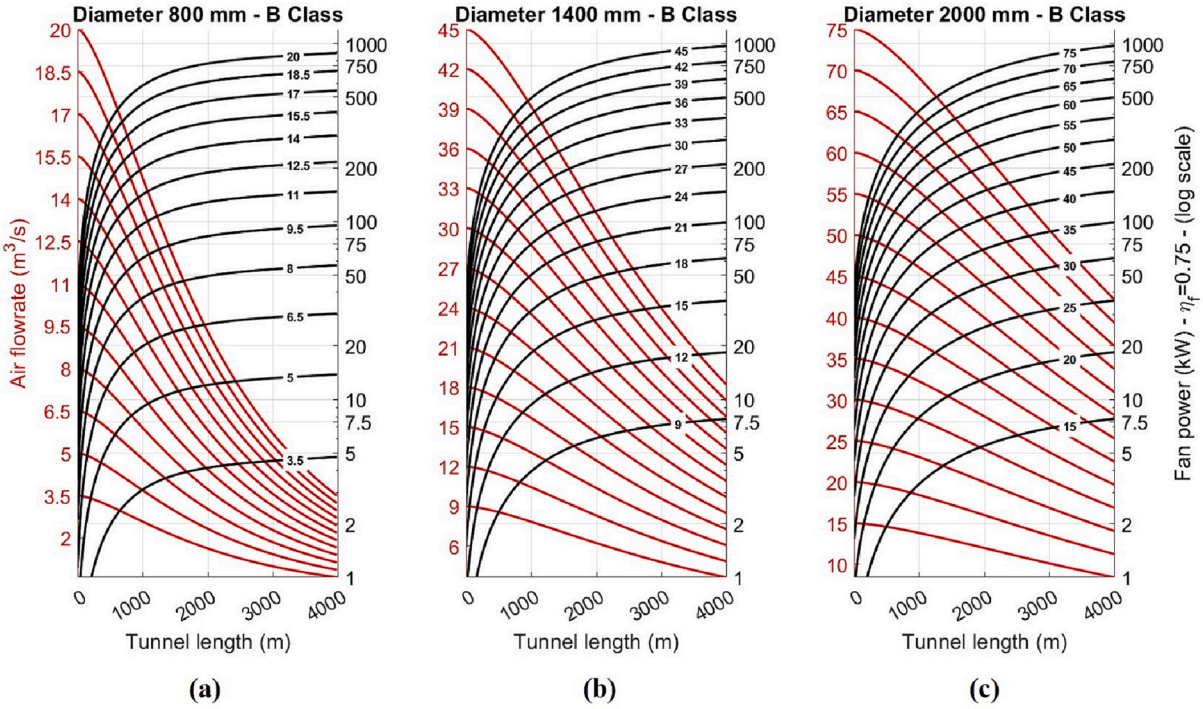


**Fig. 11.** Air leakage along the duct and fan power design for B class ducts considering tunnel lengths up to 4000 m and different duct diameters. (a) 800 mm; (b) 1400 mm; (c) 2000 mm.

and energy coefficient (∈) have been determined to estimate the power of the fan and the annual energy consumption. The power coefficient and the energy coefficient are defined as indicated in Eq. (4) and Eq. (5), respectively.

$$\xi = -log\left(\frac{\dot{W}_f \eta_f}{\rho Q_w^3}\right) \tag{4}$$

$$\in = -log\left(\frac{E_{year}\eta_T}{\rho Q_w^3 FU}\right) \tag{5}$$

where $\dot{W}_f$ is the power of the fan (kW), $\rho$ is the air density (kg m$^{-3}$), depending on the tunnel altitude, $Q_w$ is the airflow rate delivered to the working face, (m$^3$ s$^{-1}$), $\eta_f$ is the fan efficiency, $E_{year}$ is the annual energy consumption (MWh), $\eta_T$ is the global efficiency considering the auxiliary fan, motor and variable frequency drive and $FU$ is an utilization factor that depends on the daily operation time of the fan, being FU = 1 when the operation time is 24 h day$^{-1}$. Fig. 12 shows the fan power and air leakage nomogram for S class ducts considering a friction factor of 0.015 and an active leakage surface of 5 mm$^2$ m$^{-2}$. The power of the auxiliary fan can be calculated as a function of the airflow rate delivered to the working face, duct diameter, tunnel length, air density and fan efficiency. Depending on the ventilation circuit, duct diameters between 600 and 2400 mm and tunnel lengths up to 4000 m can be selected. Red lines in Fig. 12 represent the relation between the airflow supplied by the fan ($Q_f$) and the airflow delivered to the working face ($Q_w$), and black lines represent the power coefficient. Thus, from the airflow supplied by the fan, the airflow at the end of the duct can be estimated depending on the selected ducting system. Hence, the air leakage along the ventilation duct can be easily estimated as the difference between both airflow rates ($Q_f - Q_w$). Fig. 13 shows the energy consumption nomogram for S class ducts. As the fan power nomogram, duct diameters between 600 and 2400 mm and tunnel lengths up to 4000 m are considered. These parameters can be applied to most similar underground infrastructures. Note that lengths greater than 4000 m and different duct diameters can be easily resolved by applying the analytical model presented in the

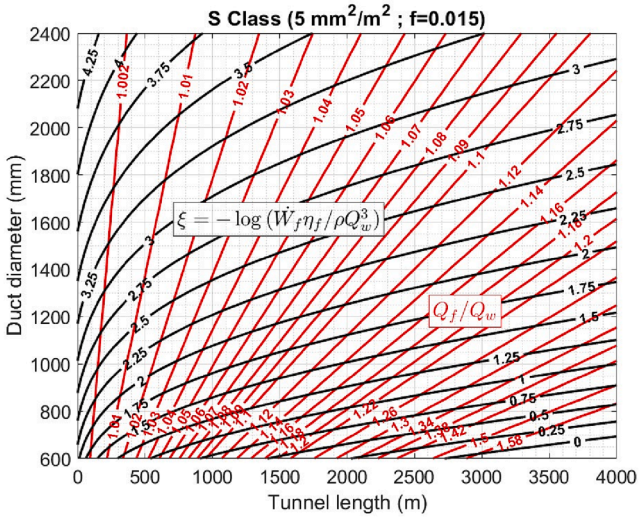


**Fig. 12.** Fan power and air leakage nomogram for S class considering duct diameters from 600 to 2400 mm and tunnel lengths up to 4000 m.

present research work, being able to size any auxiliary ventilation scenario from two novel non-dimensional variables that have been defined: power coefficient (ξ) and energy coefficient (∈). However, these situations are not recommended because higher duct diameters would be required to avoid dramatic flow rate leakages, easily higher than 50% (especially for B class scenario). Blue lines in Fig. 13 represent the energy coefficient as a function of the duct diameter and tunnel length. The nomogram represented in Fig. 13 can be used to optimize the energy efficiency and ventilation costs. Finally, from the non-dimensional variables obtained from the nomograms, the power of the fan and the annual energy consumption can be calculated by applying Eq. (6) and Eq. (7). The global efficiency $\eta_T$ is obtained as indicated in Eq. (8) as a function of the fan efficiency ($\eta_f$), motor efficiency ($\eta_{mot}$) and variable

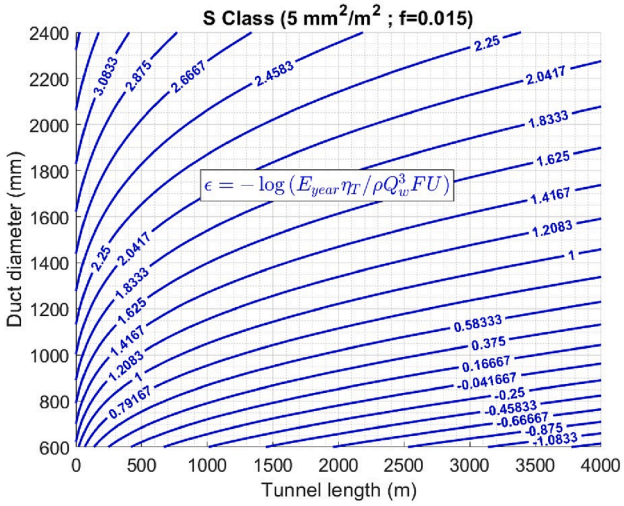


**Fig. 13.** Energy consumption nomogram for S class considering duct diameters from 600 to 2400 mm and tunnel lengths up to 4000 m.

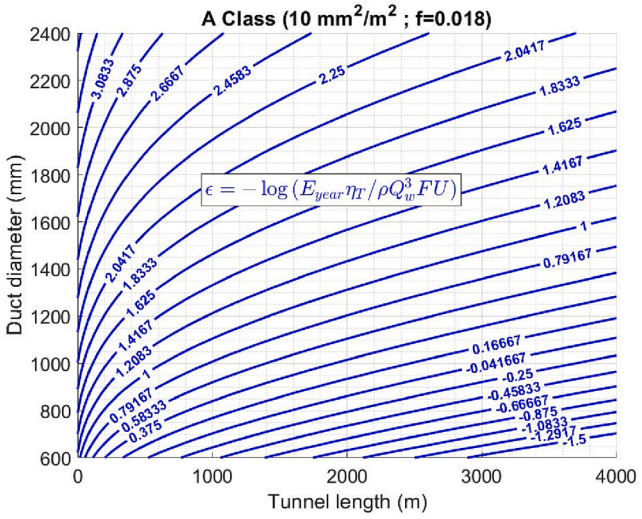


**Fig. 15.** Energy consumption nomogram for A class considering duct diameters from 600 to 2400 mm and tunnel lengths up to 4000 m.

frequency drive efficiency ($\eta_{var}$). Typical values of 0.75, 0.965 and 0.96 are generally considered for the auxiliary fan, motor and variable frequency drive efficiencies, respectively. A utilization factor of 0.83 (operation time of 20 h day$^{-1}$) is normally considered when drill and blast method is used to excavate underground infrastructures.

$$\dot{W}_f = \frac{\rho Q_w^3}{\eta_f 10^{\xi}} \tag{6}$$

$$E_{year} = \frac{\rho Q_w^3 FU}{\eta_T 10^{\epsilon}} \tag{7}$$

$$\eta_T = \eta_f \bullet \eta_{mot} \bullet \eta_{var} \tag{8}$$

The design of the auxiliary ventilation system can be carried out for A and B duct classes using the fan power and air leakage nomograms shown in Fig. 14 and Fig. 16. The values of the non-dimensional variable ξ have been determined considering friction factors of 0.018 and 0.024 and active leakage surface of 10 and 20 mm$^2$ m$^{-2}$ for A and B duct classes, respectively. Finally, energy consumption nomograms and energy coefficients for A and B duct classes are shown in Fig. 15 and Fig. 17, respectively.

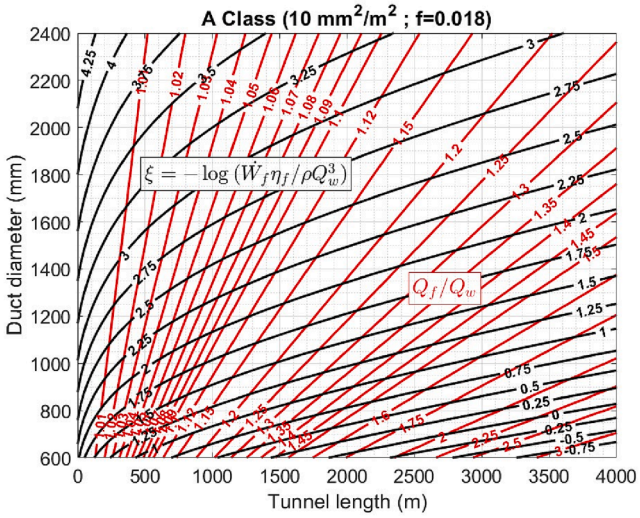


**Fig. 14.** Fan power and air leakage nomogram for A class considering duct diameters from 600 to 2400 mm and tunnel lengths up to 4000 m.

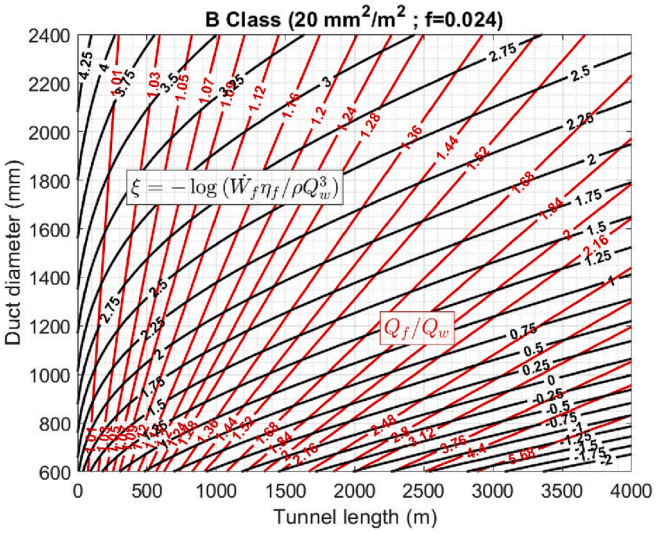


**Fig. 16.** Fan power and air leakage nomogram for B class considering duct diameters from 600 to 2400 mm and tunnel lengths up to 4000 m.

A comparative study has been carried out using the nomograms developed in the present study. A leaky ventilation duct 1000 m long has been analyzed for the three duct qualities considering an airflow rate at the working face of 25 m$^3$ s$^{-1}$, air density of 1.2 kg m$^{-3}$, fan efficiency of 0.75, motor efficiency of 0.965, variable frequency drive efficiency of 0.96 and FU = 0.83. The airflow rate at the fan discharge, non-dimensional variables, fan power, air leakage along the ducting system and annual energy consumption have been calculated considering duct diameters of 1.4 and 1.6 m. The results obtained can be observed in Table 3 and Table 4. A significant increase in fan power and air leakage has been observed for both duct diameters as duct quality worsens. The increase in fan power implies an increase in annual energy consumption, which increases from 529.32 MWh in the S-class duct to 1,017.61 MWh in the B-class duct. Increasing the duct diameter to 1.6 m, the fan power and the air leakage decrease significantly. The annual energy consumption is reduced by 48.44%, 49.16% and 50.68% for duct classes S, A and B, respectively, when the duct diameter increases from 1.4 to 1.6 m. According to the economic analysis presented in Table 5, although the cost of the duct 1.6 m in diameter is higher, due to energy

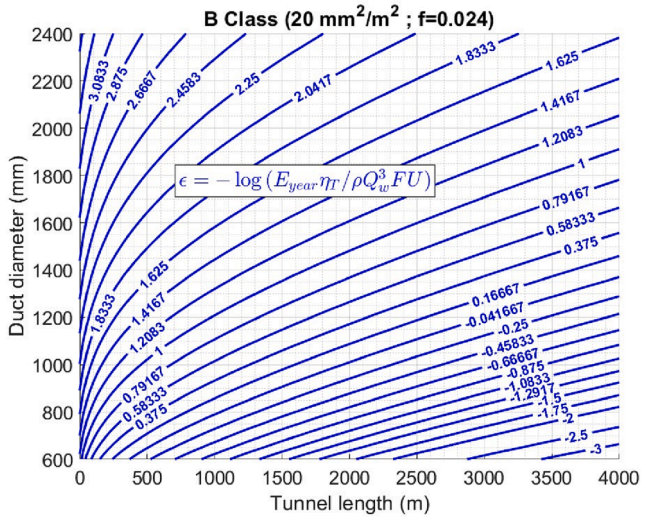


**Fig. 17.** Energy consumption nomogram for B class considering duct diameters from 600 to 2400 mm and tunnel lengths up to 4000 m.

**Table 3**
Design of auxiliary ventilation system. Leaky duct 1000 m long and 1.4 m in diameter.

| Diameter 1.4 m | S Class | A Class | B Class |
|---|---|---|---|
| $Q_f/Q_w$ | 1.030 | 1.066 | 1.156 |
| Power coefficient, ξ | 2.571 | 2.470 | 2.287 |
| Energy coefficient, ϵ | 1.628 | 1.528 | 1.344 |
| $W_f$ (kW) | 67.17 | 84.68 | 129.14 |
| $Q_f$ ($m^3\ s^{-1}$) | 25.75 | 26.66 | 28.90 |
| Air leakage ($m^3\ s^{-1}$) | 0.75 | 1.67 | 3.91 |
| $E_{year}$ (MWh) | 529.32 | 667.25 | 1,017.61 |

**Table 4**
Design of auxiliary ventilation system. Leaky duct 1000 m long and 1.6 m in diameter.

| Diameter 1.6 m | S Class | A Class | B Class |
|---|---|---|---|
| $Q_f/Q_w$ | 1.025 | 1.054 | 1.127 |
| Power coefficient, ξ | 2.858 | 2.764 | 2.594 |
| Energy coefficient, ϵ | 1.916 | 1.821 | 1.651 |
| $W_f$ (kW) | 34.63 | 43.05 | 63.69 |
| $Q_f$ ($m^3\ s^{-1}$) | 25.61 | 26.35 | 28.18 |
| Air leakage ($m^3\ s^{-1}$) | 0.61 | 1.35 | 3.17 |
| $E_{year}$ (MWh) | 272.91 | 339.22 | 501.86 |

**Table 5**
Economic analysis. B class duct 1000 m long and 1.4–1.6 m in diameter.

| Parameter | Dia. 1.4 m | Dia. 1.6 m |
|---|---|---|
| Duct cost (€) | 15,000 | 20,000 |
| Duct installation cost (€) | 22,000 | 22,000 |
| Energy consumption (MWh $year^{-1}$) | 1,017.61 | 501.86 |
| Electricity cost (€ $MWh^{-1}$) | 160 | 160 |
| Energy cost (€ $year^{-1}$) | 162,818 | 80,298 |

consumption, the ventilation costs can be significantly reduced by increasing the diameter from 1.4 to 1.6 m. Thus, the annual ventilation costs are reduced 77,520 €, representing a reduction in cost by 39%.

## 4. Conclusions

In this work, analytical and CFD numerical models have been conducted to investigate auxiliary ventilation systems with flexible ducts in tunnels and mining roadways. Air leakage and pressure drop along the duct have been analyzed considering three different duct qualities according to the Swiss Standard SIA 196 (S, A and B). In order to ensure the required airflow rate at the working face and optimize the energy efficiency and ventilation costs, the sizing of the fans and ducting system is carried out. The results obtained in the analytical model have been validated with the CFD numerical model. Good agreements were obtained between the CFD numerical approach and the analytical results.

A leaky duct 200 m long and 0.6 m in diameter has been selected as a case study in a 14 $m^2$ cross section mining roadway with an airflow rate at the working face of 10 $m^3\ s^{-1}$. The results obtained for a B class duct (typical duct class in underground excavations) indicate that the fan power reaches 103 kW with an air leakage along the ventilation duct of 0.47 $m^3\ s^{-1}$. In addition, it has also been observed that the air leakage along the ventilation duct increases when the fan total pressure increases, reducing the airflow rate at the working face. The fan power and the air leakage decrease for S and A duct classes. Increasing the duct diameter to 0.8 m, the fan power decreases down to 25 kW, representing a reduction by 75%. The ventilation system can be improved to reduce the pressure and minimize the air leakage along the duct. The connections between the duct segments could be tightened and the ruptures in the wall should be repaired.

Additionally, in order to analyze auxiliary ventilation systems for different tunnel lengths, novel nomograms have been developed to optimize the energy efficiency and ventilation costs. Two non-dimensional variables have been determined to estimate the air leakage, power of the fan and annual energy consumption. Different duct qualities, fan efficiencies, air densities and utilization factor of the fans can be selected with duct diameters between 600 and 2400 mm and tunnel lengths up to 4000 m. A case study of a tunnel 1000 m long with a duct diameter of 1.4 m and an airflow at the tunnel face of 25 $m^3\ s^{-1}$ has been selected. Using the nomograms for a B class duct, a reduction in annual ventilation costs of 39% would be obtained by increasing the diameter of the duct to 1.6 m.

The size of the tunnels and mobile equipment should be considered to select the adequate ducting system in each case. An increase in the size of the tunnel allows the installation of a larger diameter duct but significantly increases the excavation costs.

This work includes a scientific analysis combined with a novel practical application which allows for quick and reliable sizing forced ventilation systems in tunnels and mines, directly obtaining the power of the fan, the air leakage and the annual consumption of electrical energy. Therefore, the results obtained can be used by mining and tunneling engineers to design and optimize forced ventilation systems considering different fan efficiencies and air densities (tunnel altitude). Therefore, the models developed in this work allow a reliable technical and economic decision to be made, optimizing the ventilation costs. Specific friction coefficients according to the duct class and operation airflow rate and random system of holes with different diameters could be considered in future research works.

## CRediT authorship contribution statement

**Javier Menéndez:** Conceptualization, Methodology, Software, Investigation, Writing – original draft, Writing – review & editing, Visualization, Validation. **Jesús M. Fernández-Oro:** Software, Investigation, Writing – original draft, Writing – review & editing, Visualization, Validation. **Noe Merlé:** Methodology, Software, Investigation, Writing – original draft, Writing – review & editing, Visualization, Validation. **Mónica Galdo:** Software, Investigation, Visualization. **Laura Álvarez:** Methodology, Investigation, Conceptualization, Validation. **Cipriano López:** Investigation, Conceptualization, Validation. **Antonio Bernardo-Sánchez:** Investigation, Conceptualization, Validation, Supervision.

## Declaration of Competing Interest

The authors declare that they have no known competing financial interests or personal relationships that could have appeared to influence the work reported in this paper.

## Data availability

Data will be made available on request.

## References


Auld, G., 2002. Estimation of leakage in ventilation ducting. Canadian Institute of Mining Bulletin 95, 1060.

Auld, G., 2004. An estimation of fan performance for leaky ventilation ducts. Tunn. Undergr. Space Technol. 19, 539–549.

Bahrami, D., Yuan, L., Rowland, J.H., Zhou, L., Thomas, R., 2019. Evaluation of postblast re-entry times based on gas monitoring of return air. Min. Metall. Explor. 36, 513–521.

Calizaya, F., Mousset-Jones, P., 1993. A method of designing auxiliary ventilation systems for long single underground openings. In: Proceedings of the 6th US Mine Ventilation Symposium, pp. 245–250.

Calizaya, F., Mousset-Jones, P. 1994. A computer program for solving complex auxiliary ventilation systems, in SME Annual Meeting Preprint -94-206, Volume Number 94-187, Albuquerque.

Calizaya, F., Mousset-Jones, P. 1997. Estimation of leakage quantity for long auxiliary ventilation systems, in Proceedings of the 6th international mine ventilation congress, (ed. R. V. Ramani), 475–478, Littleton, CO.

Chang, X., Chai, J., Liu, Z., Qin, Y., Xu, Z., 2019. Comparison of ventilation methods used during tunnel construction. Eng. Appl. Computat. Fluid Mech. 14, 107–121.

Dang, T., Bui, D., 2020. Improving duct parameters to design auxiliary ventilation in mining roadways driven. IOP Conf. Series: Mat. Sci. Eng. 780, 032013.

Dang, P., Malanchuk, Z., Zaiets, V., 2021. Investigation of resistance and air leakage of auxiliary ventilation ducting in underground mine in Quang ninh. E3S Web Conf. 280, 08002.

De Souza, E., 2018. Cost-saving strategies in mine ventilation. Canadian Institute of Mining Journal 9 (2).

De Souza, E. 2004. Auxiliary ventilation operation practices, in Mine Ventilation: Proceedings of the 10th US/North American Mine Ventilation Symposium, (eds. R. Ganguli and S. Bandopadhyay), 341 pp., London, UK, A.A. Balkema Publishers, Taylor & Francis Routledge, May 16–19.

De Vihena, L., Margarida, J., 2020. Strategies used to control the costs of underground ventilation in some Brazilian mines. Int. Eng. J., Ouro Preto 73 (4), 555–560.

Diego, I., Torno, S., Toraño, J., Menendez, A.J., Menendez, M., Gent, M., 2011. A practical use of CFD for ventilation of underground works. Tunn. Undergr. Space Technol. 26 (1), 189–200.

Duckworth, I.J., Lowndes, I.S., 2003. Modelling of auxiliary ventilation systems. Mining Technology (Trans. Inst. Min. Metall. A) 112, 105–113.

Gupta, M., Varma, N., Sahay, N., 1987. Study of Simple auxiliary ventilation installation. Journal of Mines, Metals & Fuels 35 (8), 347–353.

Huang, R., Shen, X., Wang, B., Liao, X.P., 2020. Migration characteristics of CO under forced ventilation after excavation roadway blasting: a case study in a plateau mine. J. Clean. Prod. 267, 122094.

IEC, International Electrotechnical Commission.C 2014. IEC 60034-30-1:2014. Rotating electrical machines - Part 30-1: Efficiency classes of line operated AC motors (IE code).

Kosowski, M., Zapletal, P., Pach, G., 2022. Investigation of Forced-Air Duct Leakage Phenomenon Using CFD Methods for Underground Tunnel Construction. GeoSci. Eng. 68 (1), 58–69.

Le Roux, W. 1979. Mine ventilation notes for beginners, 3rd ed., Marshalltown, Mine Ventilation Society of South Africa.

Lee, D.K., 2011. A computational flow analysis for choosing the diameter and position of an air duct in a working face. J. Min. Sci. 47 (5), 664–667.

Lee, D.K. 2017. Evaluation of the optimum conditions for a local ventilation system in connection with the mine ventilation network. In M Hudyma¬Y Potvin (eds), UMT 2017: Proceedings of the First International Conference on Underground Mining Technology, Australian Centre for Geomechanics, Perth, pp. 655-661.

Lowndes, I.S., Crossley, A.J., Yand, Z.Y., 2004. The ventilation and climate modeling of rapid development tunnel drivages. Tunnel. Undergr. Space Technol. 19, 139–150.

McPherson, M.J. 1993. Subsurface ventilation and Environmental Engineering. Chapman & Hall, London, pp. 905.

Massanes, M., Sanmiquel, L.l., Oliva, J., 2015. Ventilation management system for underground environments. Tunn. Undergr. Space Technol. 50, 516–522.

Menéndez, J., Merle, N., Fernández-Oro, J.M., Galdo, M., Álvarez, L., Loredo, J., Bernardo-Sánchez, A., 2022. Concentration, Propagation and Dilution of Toxic Gases in Underground Excavations under Different Ventilation Modes. Int. J. Environ. Res. Public Health 19, 7092.

Millar, D., Levesque, M., Hardcastle, S., 2017. Leakage and airflow resistance in mine auxiliary ventilation ducts: effects on system performance and cost. Mining Technology 126 (1), 10–21.

Onder, N., Cevik, E., 2008. Statistical model for the volume rate reaching the end of ventilation duct. Tunn. Undergr. Space Technol. 23, 179–184.

Onder, N., Sarac, S., Cevik, E., 2006. The influence of ventilation variables on the volume rate of airflow delivered to the face of long drivages. Tunn. Undergr. Space Technol. 21, 568–574.

Onder, M. 2000. Selection of fan or fan location in ventilation of long drivages, In Proceedings of the ninth international symposium on mine planning and equipment selection, (eds. T. N. Michalakopoulos and G. N. Panagiotou), 105 pp., Rotterdam, Netherlands, Taylor & Francis, November 6–9.

Parra, M.T., Villafruela, J.M., Castro, F., Mendez, C., 2006. Numerical and experimental analysis of different ventilation systems in deep mines. Building and Environment 41, 87–93.

Pope, S. B. 2000. Turbulent Flows. University of Cambridge, Cambridge, 772 pp.

SIA 196 - Recommendation - Edition 1998, Ventilation in underground construction, Swiss Engineering and Architects Association.

Toraño, J., Torno, S., Menendez, M., Gent, M., Velasco, J., 2009. Models of methane behaviour in auxiliary ventilation of underground coal mining. Int. J. Coal Geol. 80, 35–43.

Toraño, J., Torno, S., Menendez, M., Gent, M., 2011. Auxiliary ventilation in mining roadways driven with roadheaders: Validated CFD modelling of dust behaviour. Tunn. Undergr. Space Technol. 26 (1), 201–210.

Torno, S., Toraño, J., 2020. On the prediction of toxic fumes from underground blasting operations and dilution ventilation. Conventional and numerical models. Tunn. Undergr. Space Technol. 96, 103194.

Torno, S., Toraño, J., Ulecia, M., Allende, C., 2013. Conventional and numerical models of blasting gas behaviour in auxiliary ventilation of mining headings. Tunn. Undergr. Space Technol. 34, 73–81.

Vijiapurapu, S., Cui, J., 2010. Performance of turbulence models for flows through rough pipes. Appl. Math. Model. 34, 1458–1466.

Vutukuri, V.S., 1983. Air leakage in ventilation ducting and the design of auxiliary ventilation systems. Mining Engineer 143 (262), 37–43.

Vutukuri, V. 1984. Design of auxiliary ventilation systems for long drivages, in Fifth Australian Tunneling Conference, Institution of Engineers, Australia, Sydney, Australia, October 22–24, 73 pp.

Vutukuri, V.S., 1993. An appraisal of accuracy of various formulas for the design of a simple auxiliary ventilation system. In: Proceedings, Sixth US Mine Ventilation Symposium, pp.145–150.

Wallace, K., Prosser, B., Stinnette, J.D., 2015. The practice of mine ventilation engineering. Int. J. Min. Sci. Technol. 25, 165–169.

White, F. M. 2005. Viscous Fluid Flow. New York, McGraw-Hill. 1023 pp.

S. Xin, W.H., Wang, N.N., Zhang, Zhang, C., Yuan, S., Li, H., Yang, W. 2021 Comparative studies on control of thermal environment in development headings using force/exhaust overlap ventilation systems, Journal of Building Engineering, 38, 10222.

Yi, H., Park, J., Kim, M.S., 2020. Characteristics of mine ventilation air flow using both blowing and exhaust ducts at the mining face. J. Mech. Sci. Technol. 34, 1167–1174.

Zhang, Z., Tan, Y., Zhang, H., Zhao, Y., Zhu, X., 2022. Experimental and numerical study on the influence of wall roughness on the ventilation resistance coefficient in a tunnel under construction. Tunn. Undergr. Space Technol. 119, 104198.